

Published in final edited form as:

Nature. 2014 April 24; 508(7497): 483–487. doi:10.1038/nature13203.

## Juno is the egg Izumo receptor and is essential for mammalian fertilisation

Enrica Bianchi<sup>1,2</sup>, Brendan Doe<sup>2</sup>, David Goulding<sup>2</sup>, Sanger Mouse Genetics Project<sup>2</sup>, and Gavin J. Wright<sup>1,2</sup>

<sup>1</sup>Cell Surface Signalling Laboratory, Hinxton, Cambridge, UK.

<sup>2</sup>Wellcome Trust Sanger Institute, Hinxton, Cambridge, UK.

### Abstract

Fertilisation occurs when sperm and egg recognise each other and fuse to form a new, genetically distinct organism. The molecular basis of sperm-egg recognition is unknown, but is likely to require interactions between receptor proteins displayed on their surface. Izumo1 is an essential sperm cell surface protein, but its egg receptor has remained a mystery. Here, we identify Juno as the receptor for Izumo1 on mouse eggs, and show this interaction is conserved within mammals. Female mice lacking *Juno* are infertile and *Juno*-deficient eggs do not fuse with normal sperm. Rapid shedding of Juno from the oolemma after fertilisation suggests a mechanism for the membrane block to polyspermy, ensuring eggs normally fuse with just a single sperm. Our discovery of an essential receptor pair at the nexus of conception provides opportunities for the rational development of new fertility treatments and contraceptives.

---

Fertilisation is the culminating event in sexual reproduction and requires the fusion of haploid sperm and egg to create a new, genetically distinct, diploid organism. Sperm acquire the ability to fertilise the egg within the female reproductive tract by exposing previously concealed receptor proteins onto their surface following the acrosome reaction<sup>1</sup>. Once fertilised, both the oolemma and zona pellucida are biochemically altered making the egg unreceptive to additional sperm thereby reducing the chances of creating nonviable polyploid embryos<sup>2</sup>. Several receptor proteins have been implicated in the recognition and/or fusion process<sup>3</sup>, but just two significantly affect fertility *in vivo*: Izumo1 on sperm<sup>4</sup>, and Cd9 on eggs<sup>5-7</sup>. Izumo1 (named after a Japanese marriage shrine) is redistributed to the surface of capacitated sperm<sup>8</sup>, and *Izumo1*-deficient male – but not female – mice are

---

Users may view, print, copy, and download text and data-mine the content in such documents, for the purposes of academic research, subject always to the full Conditions of use:[http://www.nature.com/authors/editorial\\_policies/license.html#terms](http://www.nature.com/authors/editorial_policies/license.html#terms)

Correspondence and requests for materials should be addressed to G.J.W. ([gw2@sanger.ac.uk](mailto:gw2@sanger.ac.uk)).

**Author contributions** E.B. and G.J.W. conceived the project, designed and analysed the experiments, and wrote the manuscript. E.B. performed all experiments with expert technical help from B.D. (ICSI injections), D.G. (electron microscopy), and the Sanger Mouse Genetics Project (transgenic mice).

**Online Content** Any additional Methods, Extended data display item and Source Data are available in the online version of the paper; references unique to these sections appear only in the online paper.

Reprints and permission information is available at [www.nature.com/reprints](http://www.nature.com/reprints).

The authors declare no competing financial interests.

Readers are welcome to comment on the online version of the paper.

infertile because sperm lacking Izumo1 cannot fuse with eggs<sup>4</sup>. Recombinant Izumo1 binds both wild-type and Cd9-deficient eggs suggesting Izumo1 interacts with an egg receptor other than Cd9<sup>9</sup>. Glycophosphatidylinositol (GPI)-anchored receptors on the egg are essential for fertilisation because removing them either enzymatically<sup>10</sup>, or genetically<sup>11</sup> renders eggs infertile. Despite these advances, the molecular basis of gamete recognition in mammals is unknown; in part, this is due to the scarcity of eggs, the challenges in solubilising membrane-embedded proteins, and the often transient nature of their extracellular interactions<sup>12</sup>. To address these challenges, we have developed techniques to identify low affinity extracellular interactions and apply them here to investigate sperm–egg recognition in mammals. We now describe the Izumo1 egg receptor as Folate receptor 4 (Folr4), a GPI-anchored protein expressed on the egg surface that is essential for female fertility. Because of its role in fertilisation and inability to bind folate, we have renamed this protein “Juno” after the Roman goddess of fertility and marriage.

## Juno is the Izumo1 receptor on oocytes

To identify an egg receptor for Izumo1, we expressed the entire ectodomain of mouse Izumo1 in mammalian cells for use as a binding probe. With the expectation that interactions with its extracellular egg receptor would be weak, we oligomerised the Izumo1 ectodomain to increase binding avidity by using a peptide sequence from a cartilage protein that forms pentamers<sup>12</sup> (Extended Data Fig. 1). The avid Izumo1 probe, but not a control protein, bound the oolemma of mouse oocytes (Fig. 1a). To determine the molecular identity of the egg binding partner for Izumo1, we used a mouse oocyte cDNA library in an iterative expression cloning approach (Extended Data Fig. 2). In each round of selection, an increasing fraction of transfected cells bound Izumo1 until three independently selected plasmid clones conferred Izumo1 binding (Fig. 1b). All three clones contained the same cDNA, encoding the Folate receptor 4 (*Folr4*) gene. Folr4 is one of three folate receptor paralogues in mouse whose main role is thought to involve folate uptake. Folr4 is expressed on CD4<sup>+</sup>CD25<sup>+</sup> regulatory T-cells in mice<sup>13</sup> and is being tested as an anti-tumour therapy<sup>13-15</sup> as well a mediator of responses to dietary folate<sup>16-18</sup>, but no functional role on oocytes has been reported. Using recombinant proteins, we showed that, unlike Folr1 and Folr2, Folr4 was unable to bind to folate (Extended Data Fig. 3a), which was expected given differences in amino acids known to be critical for folate binding<sup>19,20</sup> (Extended Data Fig. 3b). Based on this and subsequent findings, we renamed the gene encoding this protein “Juno”. Using an anti-Juno monoclonal antibody, we showed that Juno expression matched the binding pattern of the recombinant Izumo1 probe on ovulated oocytes (Fig. 1c). Preincubating oocytes with the anti-Juno antibody prevented all detectable binding of the Izumo1 probe, demonstrating that Juno is the sole Izumo1 receptor on oocytes (Fig. 1d). Similar to other folate receptor paralogues, the protein sequence of Juno suggested the presence of a C-terminal GPI-anchor site. Given the known importance of oolemmal GPI-linked proteins in fertilisation<sup>10,11</sup>, we tested whether Juno was tethered to the membrane by a GPI anchor. A large fraction of cell surface Juno staining was lost after PIPLC treatment of either HEK293 cells transfected with the *Juno* cDNA (Fig. 1e) or oocytes (Fig. 1f), demonstrating that Juno was GPI-anchored, consistent with previous results<sup>21</sup>. Taken together, these data identify Juno as the Izumo1 receptor expressed on oocytes.

## Izumo1-Juno interaction is conserved

To show that Izumo1 and Juno interacted directly, and to quantify the biophysical parameters of the interaction, we expressed and purified the entire ectodomain of Juno and measured its binding to Izumo1 using surface plasmon resonance (SPR) (Fig. 2a). Like other extracellular interactions measured using this technique, the interaction was shown to be highly transient with a  $K_D$  of  $\sim 12 \mu\text{M}$  (Extended Data Fig. 4). Juno contains a single globular domain<sup>19,20</sup> whereas Izumo1 contains both an immunoglobulin superfamily domain and a unique N-terminus termed the Izumo domain<sup>22</sup>. Consistent with the recent finding that the Izumo domain is sufficient for egg binding<sup>9</sup>, we expressed the individual domains of Izumo1, and showed, using an assay designed to detect direct low affinity extracellular protein interactions called AVEXIS<sup>23</sup>, that it is the Izumo domain that contains both the OBF13 epitope and Juno binding site (Extended Data Fig. 5). Both Izumo1 and Juno belong to small paralogous gene families which, in mouse, contain four and three members, respectively. We expressed the entire ectodomains of Izumo1, 3 and 4 (the Izumo2 paralogue did not express) and used the AVEXIS assay to systematically screen for all possible pairwise interactions with the three Folr paralogues. We observed that only mouse Izumo1 and Juno could interact (Fig. 2b). Clearly identifiable *Izumo1* and *Juno* orthologues exist in all sequenced mammalian genomes, including marsupials. To determine whether the interaction was conserved within mammals, we expressed the entire ectodomains of both Izumo1 and Juno orthologues from humans, pig (*S. scrofa*) and opossum (*M. domestica*) and assessed binding using the AVEXIS assay. Clear binding between the orthologues was observed demonstrating that the interaction is conserved within mammals (Fig. 2c).

## Juno is essential for fertilisation

To assess the role of Juno in fertilisation, we first added an anti-Juno monoclonal antibody that blocks the Izumo-Juno interaction (Fig. 1d) into *in vitro* fertilisation (IVF) assays. The anti-Juno antibody potently prevented fertilisation (Fig. 3a), with no detectable fertilisation events even when used at concentrations as low as  $0.1 \mu\text{g/mL}$  (Extended Data Fig. 6). Using similar approaches, previous research in this area has identified promising candidates for sperm-egg recognition that, when genetically deleted, have been shown to be dispensable for fertilisation<sup>3</sup>. To determine whether *Juno* was essential for fertilisation, we created *Juno*-deficient mice using embryonic stem cells disrupted at the *Juno/Folr4* locus using a gene trap allele: *Folr4<sup>tm1a(KOMP)Wtsi</sup>* (Extended Data Fig. 7). Both *Juno*<sup>-/-</sup> male and female mice developed indistinguishably from wild-type controls, showing normal rates of growth and morphology and were overtly healthy. While *Juno*<sup>-/-</sup> male and *Juno*<sup>+/-</sup> female mice were fertile, by contrast, *Juno*<sup>-/-</sup> females failed to produce any litters during three months of continuous mating with wild-type males of proven fertility (Fig. 3b). Female *Juno*<sup>-/-</sup> mice exhibited natural mating behaviours, as assessed by vaginal plug formation and the presence of motile sperm in the reproductive tract when paired with fertile wild-type males. *Juno*<sup>-/-</sup> females responded to hormone treatment by ovulating morphologically normal eggs at numbers that did not significantly differ from wild-type. *Juno*<sup>-/-</sup> eggs recovered at 0.5E after superovulation and natural mating were not fertilised and had more sperm within their perivitelline space compared to wild-type eggs, demonstrating that the zona pellucida of

*Juno*<sup>-/-</sup> eggs could be penetrated by wild-type sperm *in vivo*, which then either did not bind or fuse with the oolemma (Fig. 3c). To investigate this further, we removed the zona pellucida from *Juno*<sup>-/-</sup> eggs and found that they could not be fertilised with wild-type sperm in IVF assays, as assessed by counting the number of fused sperm and formed pronuclei per egg (Fig. 3d, e). This is consistent with a role for the Juno-Izumo1 interaction in sperm-egg adhesion or fusion. To distinguish between these possibilities, normally non-fusing HEK293 cells were separately transfected with plasmids encoding either *Juno* or *Izumo1* cDNAs and mixed. No syncytia were observed in the mixed cultures suggesting that the interaction is not sufficient for cell fusion (Extended Data Figure 8a). Furthermore, acrosome-reacted normal sperm did not bind as efficiently to zona-free Juno-deficient eggs as wild-type controls (Extended Data Figure 8b). Together, these findings suggest that the Juno-Izumo1 interaction is a necessary adhesion event between sperm and egg that is required for fertilisation.

### Juno is rapidly shed after fertilisation

After fertilisation, oocytes become largely refractory to further sperm fusion events to prevent the creation of nonviable polyploid embryos due to polyspermy. This is achieved through both a relatively slow-acting (>1 hour) hardening of the zona pellucida caused by the action of enzymes released from cortical granules after egg activation, and a faster-acting block involving biochemical changes in the oolemmal membrane. In broadcast-spawning frogs and aquatic invertebrates, the membrane block to polyspermy is very fast (a few seconds to minutes) and is achieved by electrically depolarizing the oolemma<sup>24</sup>. In mammals, the membrane block occurs over a longer timeframe (30-45 minutes), and despite being first described 60 years ago, its mechanistic basis remains a mystery<sup>2</sup>. Given the essential role of Juno in fertilisation, we explored the role it might play in establishing the membrane block to polyspermy. Interestingly, cell surface Juno was rapidly lost after fertilisation, being only weakly detectable in zona-intact fertilised eggs at telophase II and undetectable at the pronuclear stage (Fig. 4a). Similarly, Juno was barely detectable on anaphase II-stage zona-free oocytes, approximately 30 to 40 minutes after fertilisation (Extended Data Fig. 9). Folate receptors are known to take up extracellular dietary folate by endocytosis<sup>25</sup> and we therefore used immunogold electron microscopy to determine the subcellular localisation of Juno following fertilisation. To our surprise, we observed that Juno was not internalised after fertilisation but present in extracellular vesicles, presumably derived from the microvillus-rich oolemma that undergoes significant architectural changes upon fertilisation<sup>26</sup> (Fig. 4b). Some methods of fertilisation, such as intracytoplasmic sperm injection (ICSI) and parthenogenetic activation, do not lead to the establishment of an effective membrane polyspermic block<sup>2</sup>. Consistent with a role for Juno in the membrane block to polyspermy, eggs fertilised either by ICSI, or parthenogenetically-activated by ethanol, did not lose cell surface expression of Juno (Fig. 4c). The rapid shedding of Juno from the egg membrane within vesicles after fertilisation therefore provides a possible mechanism for the membrane block to polyspermy in mammalian eggs.

## Discussion

To our knowledge, the discovery of Juno as the binding partner for Izumo1 identifies these proteins as the first cell surface receptor pair essential for gamete recognition in any organism. Importantly, both female *Juno* and male *Izumo1*-deficient mice are infertile, suggesting that the interaction is essential for normal fertilisation. Comparing our findings with recent advances in the molecular understanding of cellular fusion in other biological contexts suggests that the Juno-Izumo1 interaction performs a necessary adhesion step rather than acting as a membrane “fusogen”. Unlike established fusogens such as the EFF-1 and AFF-1 proteins<sup>27</sup> or syncytins<sup>28</sup>, that are sufficient for fusion, Juno and Izumo1 do not induce the formation of syncytia when ectopically expressed on neighbouring non-fusing cells. Essential adhesion processes are required in other cellular fusion systems such as myofibre formation in both *Drosophila*<sup>29</sup> and vertebrates<sup>30</sup>, suggesting membrane fusion requires the action of other membrane proteins such as myomaker<sup>31</sup>. The expected but remarkably low *in vitro* binding affinity between soluble monomeric Juno and Izumo1 suggests that local clustering of Juno within the oolemma is important to ensure a sufficiently high binding avidity for productive interactions, a role that could be performed by the tetraspanin Cd9. Tetraspanins are known to organise other membrane proteins within microdomains<sup>32</sup> and quantitative differences in sperm adhesion to Cd9-deficient eggs have been reported<sup>33</sup>. This may also explain why female mice lacking Cd9 have reduced fertility<sup>5-7</sup>, unlike Juno-deficient mice which are completely infertile. The ability of Cd9 to organise Juno within the oolemma may be indirect since oocytes lacking Cd9 have an altered membrane architecture<sup>34,35</sup>.

Several pieces of evidence point to the rapid loss of Juno from the egg membrane after fertilisation as the mechanistic basis for the membrane block to polyspermy in mammals. Firstly, cell surface Juno is essential for fertilisation; secondly, it is undetectable on the oolemma approximately 40 minutes after fertilisation, in excellent agreement with the timing of the membrane block<sup>36</sup>; thirdly, the membrane block is both a graded response<sup>37</sup> and associated with the loss of sperm binding sites<sup>38</sup> consistent with the gradual loss of a surface receptor; and, finally, surface Juno expression is not lost in ICSI-fertilised or parthenogenetically-activated eggs that do not form an effective membrane block<sup>39</sup>. One further possibility is that because Juno is shed as vesicles after fertilisation, this creates a zone of “decoy eggs” confined within the perivitelline space that could bind to and efficiently neutralise incoming acrosome-reacted sperm to increase the potency of the sperm block. In conclusion, our discovery of an extracellular receptor pair essential for fertilisation provides a focus for the rational development of novel contraceptives and fertility treatments.

## Methods

### Generation and breeding of transgenic mice

All animal experiments were performed in accordance with local ethical and UK Home Office regulations. *Juno*-deficient mice contain a “knockout-first” allele targeted to the *Juno/Folr4* genomic locus named *Folr4<sup>tm1a(KOMP)Wtsi</sup>* and were obtained from the Knockout Mouse Project resource (KOMP-CSD ID:28054)<sup>40</sup>. Briefly, mouse ES cells

derived from C57BL/6N mice containing the correctly targeted *Juno/Folr4* locus were injected into mouse blastocysts and transplanted in pseudopregnant mice to generate chimeras. Highly (80-90 %) chimaeric males were mated with C57BL/6NTac females and germ line transmission of the targeted allele confirmed by PCR. The *tm1a* heterozygous mice were bred to obtain homozygous mice and sibling C57BL/6N wild-types were used as controls, as appropriate. Animals were genotyped using DNA extracted from ear biopsies using TaqMan® Sample-to-SNP™ Kit and used as the template for short range PCR. Wild-type and mutant alleles were amplified using the same forward primer: Juno-F: 5'-CACTGTCTGATGAGGGCCAG-3' and two different reverse primers: Juno-R 5'-AGAGCCCAGGAGGGAACAACCTC-3' for the wild-type allele, Cas-R 5'-TCGTGGTATCGTTATGCGCC-3' for the mutant allele. To rule out the possibility that the fertility defect was due to closely linked secondary mutations, a second colony of *Juno*-deficient mice were created using an independent ES cell clone targeted with the same gene trapping allele: *Folr4<sup>tm2a(KOMP)Wtsi</sup>* (KOMP-CSD ID:28055); homozygous *Juno<sup>tm2a/tm2a</sup>* mutant females were also infertile. The fertility defect was rescued by reverting the *Juno<sup>tm2a</sup>* allele essentially to a wild-type “floxed” *Juno<sup>tm2c</sup>* allele by crossing to mice that constitutively and ubiquitously express the FLPe-recombinase from the *Rosa26* locus (*Rosa26<sup>Fki</sup>* mice). Revertant homozygous (*Juno<sup>tm2c/tm2c</sup>*) eggs were fertile in IVF assays (Extended Data Fig. 7). Male and female fertility was assessed in long-term mating tests by pairing homozygous and heterozygous *Juno* adult transgenic mice with wild-type animals of proven fertility and the number of pups was monitored continuously for three months. *In vivo* fertilisation was assessed by recovered oocytes from ampullae at day 0.5E, fixed in 2 % formalin, and stained with DAPI to quantify the number of fertilised eggs. Sperm in the perivitelline space were quantified using a Leica SP5/DM6000 confocal microscope. Acro3-EGFP, acrosome reporter mice (B6;B6C3-Tg(Acro3-EGFP)01Osb)<sup>41</sup> were obtained from the RIKEN BioResource Centre.

### In vitro fertilisation

*In vitro* fertilisation was performed essentially as described<sup>42</sup>. Briefly, female mice were superovulated by injecting 5 IU of pregnant mare serum gonadotropin and 5 IU of human chorionic gonadotropin 48 hours later. Wild-type eggs were collected from the BJCB strain (CBA<Wtsi>;C57BL/6J-Jax F1) for *in vitro* fertilisation, ICSI, parthenogenetic activation and antibody staining. Eggs recovered 13 hours after hCG were freed from cumulus cells by a brief incubation in EmbryoMax M2 medium supplemented with hyaluronidase (Millipore), washed in M2 medium (Sigma) and where indicated, the zona pellucida was removed by a rapid treatment with EmbryoMax acidic Tyrode's solution (Millipore). Sperm were collected from the caudae epididymides of adult (>8 week-old) male mice and cultured for 1 h in HTF medium. *In vitro* fertilisation (IVF) assays were performed using groups of 30 to 60 eggs which were inseminated in 100 µl drops of HTF medium containing 1-2 × 10<sup>5</sup> sperm. Eggs were fixed at the indicated stage for 20 minutes with 2 % formalin in M2, and fertilisation quantified by visualization of decondensed sperm head nuclei or pronuclei formation. For antibody blocking experiments, anti-*Juno/Folr4* monoclonal antibody was added to zona-free eggs and incubated for ten minutes before adding sperm. Parthenogenetic activation of eggs was achieved by a six minute incubation in 7 % ethanol, followed by



washes in M2 medium. Eggs were then cultured for five hours to assess completion of the second meiotic division and formation of the female pronucleus.

### Intracytoplasmic sperm injection

Intracytoplasmic sperm injection (ICSI) was carried out as described<sup>43</sup> with some modifications. Epididymides were placed into 1 mL 37 °C HEPES-buffered-CZB media (H-CZB) in an Eppendorf tube and three to four incisions made to release sperm and incubated at 37 °C for 30-45 minutes to allow sperm to “swim up”. Injections were performed by first applying one or more piezo pulses to “drill” through the zona pellucida (Piezo settings, Intensity: 20, Speed: 10, Pulse: infinity) then a single piezo pulse was applied (Piezo settings, Intensity: 1-3, Speed: 1-3, Pulse: 1-3) to gently break the oolemma; finally, a single sperm head previously separated from the mid-piece and tail by piezo (Piezo settings, Intensity: 20, Speed 10, Pulse: infinity) was deposited immediately into the oocyte. Surviving oocytes were placed into a 100 µL equilibrated drop of KSOM media after “resting” for 10 minutes at room temperature. Eppendorf micromanipulators, microinjectors and a piezo actuator were used for the ICSI procedure (NK2 Transferman, Cell tram vario, Cell tram air and Piezoexpert).

### Recombinant protein production

The regions encoding the entire extracellular domains of Izumo1 and Juno orthologues were made by gene synthesis and codon optimised for expression in human cells (GenentAG). Protein sequences for Izumo1 orthologues were: mouse, *Mus musculus* (Uniprot accession number: Q9D9J7); human, *Homo sapiens* (Q8IYV9); pig, *Sus scrofa* (F1RIQ7) and opossum, *Monodelphis domestica* (H9H653). Juno/Folr4 were: mouse (Q9EQF4); human (A6ND01); pig (F1STK4); and opossum (F7AHC3). Mouse Izumo and Juno paralogues were: Izumo2 (Q9DA16), Izumo3 (A6PWV3), Izumo4 (D3Z690), Folr1 (P35846), and Folr2 (Q05685). The rat Cd200 and Cd200R were used for positive controls as described<sup>44</sup>. All ectodomains were flanked by unique NotI and AscI sites that were used to clone them into protein expression vectors that encoded either biotinylated ‘baits’ or pentameric FLAG-tagged ‘preys’<sup>45</sup>. An expression construct produced in exactly the same manner containing the Izumo2 paralogue did not produce any protein in several independent transfections. The Izumo and Ig-like domain fragments were amplified from the entire ectodomain construct by PCR and either cloned into the normal biotinylated “bait” vector (Izumo domain) or a vector that contained an exogenous signal peptide (Ig-like domain)<sup>46</sup>. Proteins were expressed as secreted proteins in HEK293E cells<sup>47</sup>.

### Expression cloning

The Izumo1 receptor was identified by an expression cloning method as described<sup>48</sup>, using a normalized mouse oocyte cDNA library (NIH\_MGC\_257\_N, Express Genomics, USA). Initial sequencing of randomly-selected clones confirmed that the library contained a good fraction of unique full-length cDNAs: 130/161 (81 %) of randomly sequenced plasmids were unique, and 18 % were full-length as determined by the presence of the start methionine and stop codon. The cDNA library was plated at a density of ~100 colonies/plate and pools of purified plasmids were transfected using Lipofectamine 2000 (Invitrogen) into

HEK293T cells (ATCC Cat. No. CRL-3216) grown as adherent monolayers in flat-bottomed 48-well microtitre plates. After 48 hours, cells were incubated with the FLAG-tagged Izumo binding probe for 30 minutes, washed, fixed with a 4 % formalin solution and stained with an anti-FLAG Cy3 (Sigma). Wells were manually inspected for Izumo1 staining with an epifluorescence microscope and plasmid pools that resulted in positive Izumo1 staining were used to transform DH5 $\alpha$  *E. Coli*. Plasmids were purified from individual colonies grown in 96-well blocks, pooled into groups of twelve, and HEK293T cells again transfected and tested for Izumo1 binding 48 hours later as described above. A final round of Izumo1 staining was performed with individual plasmids from the positive pools to identify three independent positive clones which were sequenced using Sanger dideoxy sequencing to identify Folr4 which was renamed Juno.

### Staining mouse eggs with avid recombinant proteins and antibodies

To detect the Izumo1 probe binding to the oolemma, purified pentamerized FLAG-tagged Izumo1 was added to unfixed eggs. After 30 minutes at 37 °C, eggs were fixed with 2 % formalin, washed, and stained with anti-Flag-Cy3 antibody diluted 1:500 in M2 media. Izumo1 binding to HEK293T cells was detected using the same method except that protein and antibody were diluted in PBS/2 % BSA. Juno was detected on eggs fixed with 2 % formalin using the anti-Juno/Folr4 monoclonal antibody diluted to 2  $\mu$ g/mL in M2 media, washed, followed by an anti-rat Alexa Fluor 488. Stained eggs were mounted on a microscope glass in SlowFade with DAPI (Molecular Probes). Samples were analysed with Leica SP5/DM6000 confocal microscope.

### Extracellular protein interaction screening by AVEXIS

Bait and prey proteins were normalised to activities suitable for the AVEXIS assay as described<sup>49</sup>. Biotinylated baits that had been either purified or dialysed against HBS were immobilised in streptavidin-coated 96-well microtitre plates (NUNC). Preys were incubated for two hours, washed 3x HBS/0.1 % Tween-20, 1x HBS and 125  $\mu$ g/mL of nitrocefin added, and absorbance values measured at 485 nm on a Pherastar plus (BMG laboratories). A protein consisting of the Cd4d3+4 tag alone was used as a negative control bait and a biotinylated anti-Cd4 monoclonal antibody (anti-prey) used as a positive control as required. The mouse Izumo1-Juno interaction has been repeated more than three times in the laboratory by AVEXIS using independent protein preparations; importantly, the interaction is observed if the Izumo1 or Juno proteins are presented as either the bait or prey. Similarly, the Izumo1-Juno interactions from different mammalian species were repeatable and independent of the bait-prey orientation.

### Antibodies

Antibodies were obtained from the following suppliers: mouse anti-rat Cd4d3+4, clone OX68 (AbD Serotec), rat anti-mouse Folr4/Juno, clone TH6 (BioLegend), Armenian hamster anti-mouse Cd55, clone RIKO-3 (BioLegend), rat anti-trinitrophenol+KLH IgG<sub>2b</sub> isotype control (BioLegend), anti-FLAG-Cy3 conjugated (Sigma), anti-rat AlexaFluor 488 and 568 (Molecular Probes), mouse anti-mouse Izumo1 OBF13 was a kind gift from N. Inoue and M. Okabe (Osaka University).



## Surface plasmon resonance

Protein interactions were quantified by surface plasmon resonance studies as implemented in a Biacore T100 instrument (GE Healthcare). Briefly, biotinylated proteins were immobilised on a streptavidin-coated sensor chip. Approximately 450 RU of rat Cd4d3+4 was used as a reference and approximate molar equivalents of biotinylated mouse Izumo1Cd4d3+4 protein immobilised in the query flow cell. Purified mouse JunoCd4d3+4-6His protein was resolved by gel filtration just prior to SPR experiments to remove any aggregated protein which influence the measurement of kinetic parameters. Increasing concentrations of purified JunoCd4d3+4-6His was injected at 10  $\mu\text{L}/\text{min}$  for equilibrium measurements whereas high flow rates (100  $\mu\text{L}/\text{min}$ ) were used for kinetic measurements to reduce the confounding effects of analyte rebinding. Although essentially all the bound Juno dissociated during the wash-out phase, the surface was “regenerated” with a pulse of 2M NaCl at the end of each cycle. Equilibrium binding measurements were taken once equilibrium had been reached using reference-subtracted sensorgrams. Duplicate injections of the same concentration of JunoCd4d3+4-6His in each experiment were superimposable demonstrating no loss of activity after regenerating the surface. Both kinetic and equilibrium binding data were analysed in the manufacturer’s Biacore T100 evaluation software (GE Healthcare) and all experiments were performed at 37 °C.

## Enzyme-linked immunosorbant assay (ELISA) and Western blotting

Biotinylated proteins were captured on streptavidin-coated plates for one hour before adding 10  $\mu\text{g}/\text{mL}$  primary antibody for 90 minutes. Plates were washed in HBS/0.1 % Tween-20 (HBST) before adding the appropriate secondary antibody conjugated to alkaline phosphatase (Sigma). Plates were washed 3x HBST and 1x HBS before adding 100  $\mu\text{L}$  *p*-nitrophenyl phosphate (Sigma 104 alkaline phosphatase substrate) at 1 mg/mL in diethanolamine buffer. Absorbance readings were taken at 405 nm on a Pherastar plus (BMG laboratories). Where appropriate, proteins were denatured by heat treatment at 90 °C for 10 mins. ELISAs were performed at room temperature.

Western blotting was performed essentially as described<sup>50</sup>. Briefly, secreted biotinylated Izumo1 domains were normalised and resolved under non-reducing conditions by SDS-PAGE and blotted to Hybond-P PVDF membrane (GE Healthcare) for 2 hours at 30 V. After blocking for 1 h with 2 % BSA, the membrane was incubated for 1 h with OBF13 diluted 1:200 in PBST/2 % BSA, washed three times and incubated with an HRP-conjugated anti-mouse antibody. Proteins were detected using SuperSignal West Pico Chemiluminescent substrate (Thermo Scientific).

## Folate binding assays

Endogenous folate was first dissociated from its receptor and adsorbed to activated charcoal by incubating the biotinylated proteins for 20 minutes at 4 °C in 250 mM NaCl, 25 mM sodium acetate, 1 % Triton X-100, 15 % FBS and 40 mg/mL charcoal, pH 3.5 as described<sup>20</sup>. After centrifugation, the solution was adjusted to pH 7.4 and the proteins were captured on streptavidin-coated plates for one hour. Folic acid conjugated to horseradish peroxidase (HRP) (C057 CalBioagents, USA) was diluted 1:150 in 25 mM Tris pH 8.0, 150 mM NaCl, 0.1 % Triton X-100, and incubated for 1 hour. Finally, the plates were

washed, 100  $\mu$ L of Ultra-TMB substrate (Pierce Biotechnology) was added and absorbance readings were taken after 45 minutes.

### PIPLC treatment

Zona-free metaphase-II eggs or HEK293 cells transfected with an expression construct encoding full length *Juno* were treated with PIPLC (Sigma) for 30 minutes at 37 °C in HTF medium, washed and fixed with a 2 % formalin solution. The presence of Juno was determined using the anti-Juno/Folr4 antibody using either immunocytochemistry by confocal microscopy (eggs) or flow cytometry (transfected HEK cells) on a BD Biosciences LSR Fortessa cell analyser and data analysed using FACSDiva software.

### Juno immunogold electron microscopy

Eggs were resuspended in a 4 % paraformaldehyde / 0.2 % glutaraldehyde mixture in PBS for one hour (all steps at room temperature), washed three times in PBS, blocked with PBS/glycine followed by 5 % foetal calf serum for 30 minutes and then incubated in rat anti-Juno for 1 hour. After rinsing, the eggs were incubated with goat anti-rat secondary antibody conjugated to ultra-small (0.8 nm) gold particles for 30 minutes, washed, and fixed in 1.5 % glutaraldehyde for 30 minutes, rinsed in distilled water and then signals amplified with a silver enhancing kit (Amersham IntenSE M) for 10 minutes. The eggs were post-fixed in 1 % osmium tetroxide for 30 minutes, dehydrated in an ethanol series and embedded in TAAB resin. 60 nm ultrathin sections were cut on a Leica UC6 ultramicrotome, contrasted with uranyl acetate and lead citrate and examined on a 120kV FEI Spirit Biotwin using a Tietz F4.15 CCD camera.

### Cellular binding/fusion assay using ectopic expression

HEK293T cells were transfected with plasmids encoding mouse *Juno* (clone B2 from the cDNA library) or with GFP-tagged full-length mouse *Izumo1* (clone MG222708, Origene, USA) using Lipofectamine 2000 (Invitrogen) according to the manufacturer's protocol. The day after transfection, equal numbers of cells were mixed and examined for binding and fusion using confocal microscopy two and 24 hours later. *Izumo1* was detected by the GFP tag and Juno using the anti-Juno antibody by immunocytochemistry. Briefly, cells were incubated with anti- Juno antibody, diluted 1:200 in PBS/2 % BSA, washed in PBS followed by anti-rat Alexa Fluor 568-conjugated secondary antibody (Molecular Probes). Finally, nuclei were stained with DAPI (Slow Fade mounting medium, Molecular Probes).

### Supplementary Material

Refer to Web version on PubMed Central for supplementary material.

### Acknowledgements

This work was supported by the Wellcome Trust grant number [098051]. We thank: William Skarnes and James Bussell for advice on transgenic mouse generation and breeding; Jason Kerr for construct design; Allan Bradley and Luca Jovine for helpful comments on the manuscript; and Masaru Okabe and Naokazu Inoue for the OBF13 antibody.

## References

1. Okabe M. The cell biology of mammalian fertilization. *Development*. 2013; 140:4471–4479. [PubMed: 24194470]
2. Gardner AJ, Evans JP. Mammalian membrane block to polyspermy: new insights into how mammalian eggs prevent fertilisation by multiple sperm. *Reprod Fertil Dev*. 2006; 18:53–61. [PubMed: 16478602]
3. Ikawa M, Inoue N, Benham AM, Okabe M. Fertilization: a sperm's journey to and interaction with the oocyte. *J Clin Invest*. 2010; 120:984–994. [PubMed: 20364096]
4. Inoue N, Ikawa M, Isotani A, Okabe M. The immunoglobulin superfamily protein Izumo is required for sperm to fuse with eggs. *Nature*. 2005; 434:234–238. [PubMed: 15759005]
5. Le Naour F, Rubinstein E, Jasmin C, Prenant M, Boucheix C. Severely reduced female fertility in CD9-deficient mice. *Science*. 2000; 287:319–321. [PubMed: 10634790]
6. Miyado K, et al. Requirement of CD9 on the egg plasma membrane for fertilization. *Science*. 2000; 287:321–324. [PubMed: 10634791]
7. Kaji K, et al. The gamete fusion process is defective in eggs of Cd9-deficient mice. *Nat Genet*. 2000; 24:279–282. [PubMed: 10700183]
8. Satouh Y, Inoue N, Ikawa M, Okabe M. Visualization of the moment of mouse sperm-egg fusion and dynamic localization of IZUMO1. *J Cell Sci*. 2012; 125:4985–4990. [PubMed: 22946049]
9. Inoue N, et al. Molecular dissection of IZUMO1, a sperm protein essential for sperm-egg fusion. *Development*. 2013; 140:3221–3229. [PubMed: 23824580]
10. Coonrod SA, et al. Treatment of mouse oocytes with PI-PLC releases 70-kDa (pI 5) and 35- to 45-kDa (pI 5.5) protein clusters from the egg surface and inhibits sperm-oolemma binding and fusion. *Dev Biol*. 1999; 207:334–349. [PubMed: 10068467]
11. Alfieri JA, et al. Infertility in female mice with an oocyte-specific knockout of GPI-anchored proteins. *J Cell Sci*. 2003; 116:2149–2155. [PubMed: 12692150]
12. Wright GJ. Signal initiation in biological systems: the properties and detection of transient extracellular protein interactions. *Mol Biosyst*. 2009; 5:1405–1412. [PubMed: 19593473]
13. Yamaguchi T, et al. Control of immune responses by antigen-specific regulatory T cells expressing the folate receptor. *Immunity*. 2007; 27:145–159. [PubMed: 17613255]
14. Teng MW, et al. Multiple antitumor mechanisms downstream of prophylactic regulatory T-cell depletion. *Cancer Res*. 2010; 70:2665–2674. [PubMed: 20332236]
15. Liang SC, Moskalenko M, Van Roey M, Jooss K. Depletion of regulatory T cells by targeting folate receptor 4 enhances the potency of a GM-CSF-secreting tumor cell immunotherapy. *Clin Immunol*. 2013; 148:287–298. [PubMed: 23811319]
16. Kunisawa J, Hashimoto E, Ishikawa I, Kiyono H. A pivotal role of vitamin B9 in the maintenance of regulatory T cells in vitro and in vivo. *PLoS One*. 2012; 7:e32094. [PubMed: 22363800]
17. Kinoshita M, et al. Dietary folic acid promotes survival of Foxp3+ regulatory T cells in the colon. *J Immunol*. 2012; 189:2869–2878. [PubMed: 22869901]
18. Salbaum JM, Kruger C, Kappen C. Mutation at the folate receptor 4 locus modulates gene expression profiles in the mouse uterus in response to periconceptional folate supplementation. *Biochim Biophys Acta*. 2013; 1832:1653–1661. [PubMed: 23651732]
19. Chen C, et al. Structural basis for molecular recognition of folic acid by folate receptors. *Nature*. 2013; 500:486–489. [PubMed: 23851396]
20. Wibowo AS, et al. Structures of human folate receptors reveal biological trafficking states and diversity in folate and antifolate recognition. *Proc Natl Acad Sci U S A*. 2013; 110:15180–15188. [PubMed: 23934049]
21. Jia Z, et al. A novel splice variant of FR4 predominantly expressed in CD4+CD25+ regulatory T cells. *Immunol Invest*. 2009; 38:718–729. [PubMed: 19860584]
22. Ellerman DA, et al. Izumo is part of a multiprotein family whose members form large complexes on mammalian sperm. *Mol Reprod Dev*. 2009; 76:1188–1199. [PubMed: 19658160]

23. Bushell KM, Sollner C, Schuster-Boeckler B, Bateman A, Wright GJ. Large-scale screening for novel low-affinity extracellular protein interactions. *Genome Res.* 2008; 18:622–630. [PubMed: 18296487]
24. Jaffe LA. Fast block to polyspermy in sea urchin eggs is electrically mediated. *Nature.* 1976; 261:68–71. [PubMed: 944858]
25. Sabharanjak S, Mayor S. Folate receptor endocytosis and trafficking. *Adv Drug Deliv Rev.* 2004; 56:1099–1109. [PubMed: 15094209]
26. Jackowski S, Dumont JN. Surface alterations of the mouse zona pellucida and ovum following in vivo fertilization: correlation with the cell cycle. *Biol Reprod.* 1979; 20:150–161. [PubMed: 454729]
27. Podbilewicz B, et al. The *C. elegans* developmental fusogen EFF-1 mediates homotypic fusion in heterologous cells and in vivo. *Dev Cell.* 2006; 11:471–481. [PubMed: 17011487]
28. Mi S, et al. Syncytin is a captive retroviral envelope protein involved in human placental morphogenesis. *Nature.* 2000; 403:785–789. [PubMed: 10693809]
29. Abmayr SM, Pavlath GK. Myoblast fusion: lessons from flies and mice. *Development.* 2012; 139:641–656. [PubMed: 22274696]
30. Powell GT, Wright GJ. Jamb and jamc are essential for vertebrate myocyte fusion. *PLoS Biol.* 2011; 9:e1001216. [PubMed: 22180726]
31. Millay DP, et al. Myomaker is a membrane activator of myoblast fusion and muscle formation. *Nature.* 2013; 499:301–305. [PubMed: 23868259]
32. Hemler ME. Tetraspanin functions and associated microdomains. *Nat Rev Mol Cell Biol.* 2005; 6:801–811. [PubMed: 16314869]
33. Jegou A, et al. CD9 tetraspanin generates fusion competent sites on the egg membrane for mammalian fertilization. *Proc Natl Acad Sci U S A.* 2011; 108:10946–10951. [PubMed: 21690351]
34. Runge KE, et al. Oocyte CD9 is enriched on the microvillar membrane and required for normal microvillar shape and distribution. *Dev Biol.* 2007; 304:317–325. [PubMed: 17239847]
35. Zylkiewicz E, Nowakowska J, Maleszewski M. Decrease in CD9 content and reorganization of microvilli may contribute to the oolemma block to sperm penetration during fertilization of mouse oocyte. *Zygote.* 2010; 18:195–201. [PubMed: 19939329]
36. Wolf DP. The block to sperm penetration in zona-free mouse eggs. *Developmental Biology.* 1978; 64:1–10. [PubMed: 566228]
37. Gardner AJ, Williams CJ, Evans JP. Establishment of the mammalian membrane block to polyspermy: evidence for calcium-dependent and -independent regulation. *Reproduction.* 2007; 133:383–393. [PubMed: 17307906]
38. Horvath PM, Kellom T, Caulfield J, Boldt J. Mechanistic studies of the plasma membrane block to polyspermy in mouse eggs. *Mol Reprod Dev.* 1993; 34:65–72. [PubMed: 8418819]
39. Wortzman-Show GB, Kurokawa M, Fissore RA, Evans JP. Calcium and sperm components in the establishment of the membrane block to polyspermy: studies of ICSI and activation with sperm factor. *Mol Hum Reprod.* 2007; 13:557–565. [PubMed: 17575288]
40. Skarnes WC, et al. A conditional knockout resource for the genome-wide study of mouse gene function. *Nature.* 2011; 474:337–342. [PubMed: 21677750]
41. Nakanishi T, et al. Real-time observation of acrosomal dispersal from mouse sperm using GFP as a marker protein. *FEBS Lett.* 1999; 449:277–283. [PubMed: 10338148]
42. Nagy, A. *Manipulating the Mouse Embryo: A Laboratory Manual.* 3rd edn. Cold Spring Harbor Laboratory Press; 2003.
43. Kimura Y, Yanagimachi R. Intracytoplasmic sperm injection in the mouse. *Biol Reprod.* 1995; 52:709–720. [PubMed: 7779992]
44. Sun Y, Gallagher-Jones M, Barker C, Wright GJ. A benchmarked protein microarray-based platform for the identification of novel low-affinity extracellular protein interactions. *Anal Biochem.* 2012; 424:45–53. [PubMed: 22342946]

## Methods references

45. Martin S, et al. Construction of a large extracellular protein interaction network and its resolution by spatiotemporal expression profiling. *Mol Cell Proteomics*. 2010; 9:2654–2665. [PubMed: 20802085]
46. Crosnier C, et al. A Library of Functional Recombinant Cell-surface and Secreted *P. falciparum* Merozoite Proteins. *Mol Cell Proteomics*. 2013; 12:3976–3986. [PubMed: 24043421]
47. Durocher Y, Perret S, Kamen A. High-level and high-throughput recombinant protein production by transient transfection of suspension-growing human 293-EBNA1 cells. *Nucleic Acids Res*. 2002; 30:E9. [PubMed: 11788735]
48. Golemis, EA. *Protein-protein Interactions: A Molecular Cloning Manual*. Cold Spring Harbor Laboratory Press; 2001.
49. Kerr JS, Wright GJ. Avidity-based extracellular interaction screening (AVEXIS) for the scalable detection of low-affinity extracellular receptor-ligand interactions. *J Vis Exp*. 2012:e3881. [PubMed: 22414956]
50. Bartholdson SJ, et al. Semaphorin-7A is an erythrocyte receptor for *P. falciparum* merozoite-specific TRAP homolog, MTRAP. *PLoS Pathog*. 2012; 8:e1003031. [PubMed: 23166499]

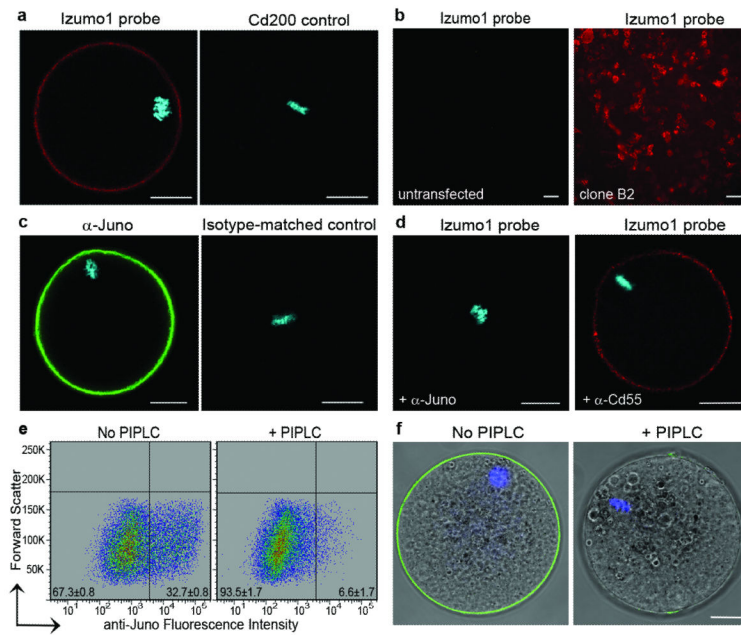


**Figure 1. Juno is the GPI-anchored oocyte surface receptor for Izumo1**

(a) An avid recombinant Izumo1 protein but not a control bound the oolemma. (b) Izumo1 bound HEK293 cells transfected with a *Juno* cDNA (clone B2) but not untransfected controls. (c) Juno is highly expressed on the oolemma of unfertilised eggs. (d) Preincubation of eggs with an anti-Jun0 but not an anti-Cd55 control antibody blocked binding of recombinant Izumo1 protein. (e, f) Cell surface Juno was lost after treatment with PIPLC on *Juno*-transfected HEK293 cells (e) or eggs (f). Images are single optical sections of unfertilised mouse metaphase II eggs; scale bars are 20  $\mu\text{m}$  in a, c, d, f, and 10  $\mu\text{m}$  in b.



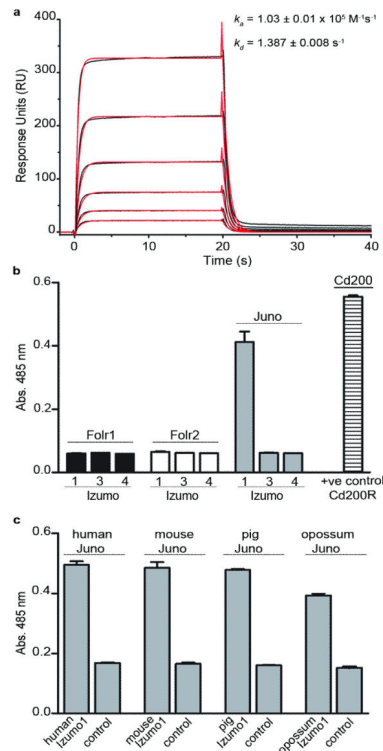


**Figure 2. The Juno-Izumo1 interaction is direct, transient and conserved across mammals**

**(a)** Biophysical analysis of the Juno-Izumo1 interaction using SPR. Serial dilutions of purified, soluble Juno were injected over immobilised Izumo1, and kinetic parameters derived from a 1:1 Langmuir binding model (red lines). **(b)** Binding specificity within the paralogues of the mouse Izumo and Folr families: only Juno (Folr4) bound Izumo1. **(c)** The Juno-Izumo1 interaction is conserved across mammals. AVEXIS was used for binding analysis in **(b)** and **(c)** using recombinant Folr/Juno proteins as preys and Izumo proteins as baits; control bait in **(c)** was Cd4. All bar charts show mean  $\pm$  SEM;  $n = 3$ .

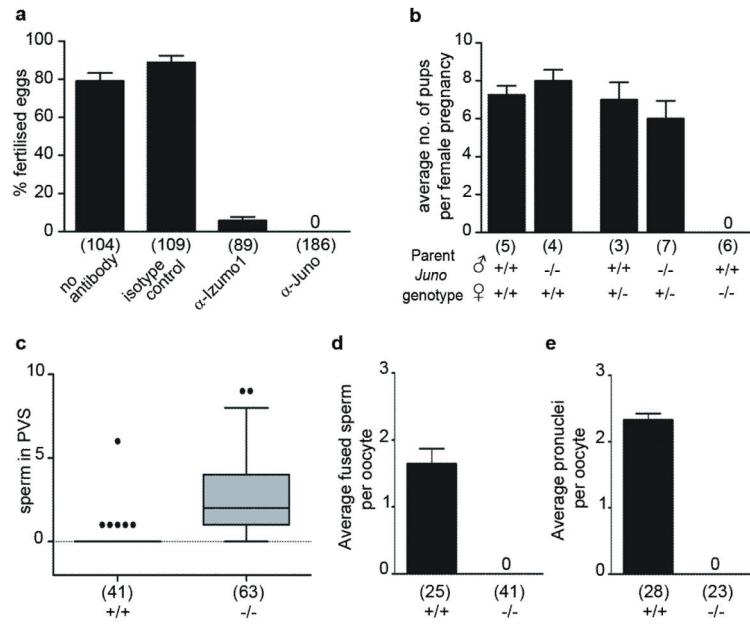


### Figure 3. *Juno* is essential for female fertility

(a) An anti-*Juno* monoclonal antibody potently blocked *in-vitro* fertilisation; anti-Izumo1 is shown for comparison. (b) Female *Juno*<sup>-/-</sup> mice are infertile. Continuous mating of *Juno*<sup>-/-</sup> female mice to proven wild-type males for three months did not result in any pups. (c) Greater numbers of sperm were observed in the perivitelline space (PVS) of eggs from superovulated *Juno*-deficient (-/-) mice relative to wild-type (+/+). (d, e) *Juno*<sup>-/-</sup> eggs do not fuse with wild-type sperm *in vitro*. Sperm were added to *Juno*-deficient (-/-) and wild-type (+/+) eggs and fused sperm quantified after two hours (d), or pronuclei after six hours (e). All bar charts show mean  $\pm$  SEM; numbers in parentheses are total number of eggs (a, c, d, e) or number of mating pairs (b).

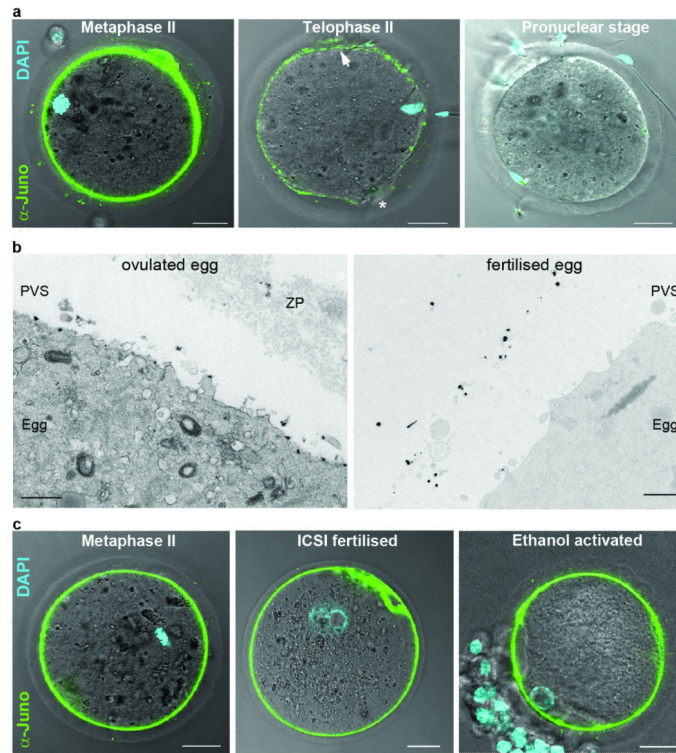


**Figure 4. Normally-fertilised, but not ICSI-fertilised or parthenogenetically-activated eggs, rapidly shed Juno from the oolemma**

(a) Cell surface Juno rapidly becomes undetectable after fertilisation. Juno (green) is expressed on ovulated metaphase II eggs but is barely evident at telophase II and undetectable on pronuclear-stage zygotes. Arrow and asterisk indicate sites of first and second polar body extrusion respectively; chromosomes are not within the plane of focus. (b) Immunogold electron microscopy localised Juno primarily to the oolemma in unfertilised, ovulated eggs but was redistributed to vesicles within the perivitelline space within one hour after fertilisation. (c) Eggs fertilised by ICSI or parthenogenetically-activated retain oolemmal Juno staining until at least the pronuclear stage, as shown. Nuclei/pronuclei were visualised with DAPI (blue). Images show representative eggs from three independent experiments. Scale bars represent 20  $\mu\text{m}$  (a and c) and 1  $\mu\text{m}$  (b).